

Statistical properties of a granular gas fluidized by turbulent air wakes

Miguel A. López-Castaño ✉, Juan F. González-Saavedra, Álvaro Rodríguez-Rivas, and Francisco Vega Reyes

Departamento de Física and Instituto de Computación Científica Avanzada (ICCAEx), Universidad de Extremadura, 06071 Badajoz, Spain
malopez00@unex.es

Abstract. We perform experiments with a granular system that consists of a collection of identical hollow spheres (ping-pong balls). Particles rest on a horizontal metallic grid and are confined within a circular region. Fluidization is achieved by means of a turbulent air current coming from below. Air flow is adjusted so that the balls do not elevate over the grid, as an approach to 2D dynamics. With a high-speed camera, we take images of the system. From these images we can infer horizontal particle positions and velocities by means of particle-tracking algorithms. With the obtained data we analyze: a) the systematic measurement error in the determination of positions and velocities from our digital images; b) the degree of homogeneity achieved in our experiments (which depends on possible deviations of the grid from the horizontal and on the homogeneity of turbulent air wakes). Interestingly, we have observed evidences of crystallization at high enough densities.

1 Introduction

Experimental works on the symmetry properties of nearly close-packed particles were carried out in the early 20th for direct visualization of the crystal structure in laboratory scale model systems (by that time this was technically not possible for real solid crystals). Pioneering work by L. Bragg and J. F. Nye in experiments with soap bubbles monolayers [5], which clearly reported a macroscopic hexagonal crystal structure, was followed by other interesting analogous works on different phases in systems with macroscopic particles [9,8,7].

The present work was conceived as an approach to this kind of experimental works. Our laboratory set-up is directly inspired in the work by Durian and co-workers, who analyzed the properties of Brownian motion in a macroscopic particle [14]; a ping pong ball fluidized by turbulent air wakes. These wakes are produced at the Von Kármán streets due to air flow past a spherical particle [21]. We built a very similar set-up, this time using $\sim 10^2$ particles in most of our experiments. The final aim of our series of measurements is to search for eventual phase transitions, in analogy with the observations in thin vibrated layers [15].

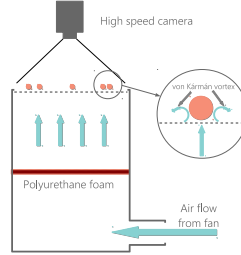


Fig. 1. Sketch of the experimental set-up

2 Description of the system

We perform experiments with a variable number N of identical spherical particles. Specifically, our particles are ping-pong balls with diameter $\sigma = 4$ cm (ARTENGO[®] brand balls, made of ABS plastic, this material having a mass density $\rho \simeq 0.08$ g cm⁻³). Particles rest on a metallic mesh (circular holes of 3 mm diameter arranged in a triangular lattice) and are enclosed by a circular wall made of polylactic acid (PLA). The diameter of this circular boundary is $D = 72.5$ cm and its height is $h \simeq 4.5$ cm $> \sigma$. Thus, the total area of the system available to the spheres is $A = 0.413$ m² $= 328.65 \times \pi(\sigma/2)^2$, which means that up to $N_{\max} = 0.9069 \times 328.65 \simeq 298$ balls can fit in our system, if we ignore boundary effects (which would reduce this number). The grid is mounted and carefully levelled so that it remains as horizontal as possible (i.e.; perpendicular to gravity). In this way, we expect to achieve dynamics in which gravity does not create any anisotropy in the system behaviour.

Steady dynamics of the particulate system is achieved by means of a vertical air current coming from below, as depicted in Figure 1. We use for this a fan, model SODECA[®] HCT-71-6T-0.75/PL, that is able to produce air current intensities u_{air} passing through the metallic grid plane with rates in the range of [2 - 5.5] m/s. An intermediate foam (~ 2 cm thick) homogenizes the air current from the fan. The air flow distribution over the grid was measured using a turbine digital anemometer, plugged to a computer to collect data. We observed that the air current flow suffers local deviations over the grid of less than 10%, with respect to the average u_{air} .

The air flow coming from the fan produces turbulent wakes past the spheres [21]. Air current intensity is adjusted so that particles never levitate, and remain in contact with the metallic grid at all times. With this, we achieve a particle dynamics that is effectively two-dimensional, since the relevant particle motion is contained within the grid plane.

Summarizing, we built a set-up that has the following properties: 1) It is a many-particle system; 2) the energy input is homogeneous; 3) the dynamics is contained in a horizontal plane (the grid) and as a consequence gravity does not

introduce a predominant direction; 4) symmetry-break is observed in the form of a hexagonal arrangement of the particles.

A series of experiments has been carried out, by modifying the values of air flow intensity ($2 \text{ m/s} \leq u_{air} \leq 5.5 \text{ m/s}$) and packing fraction $\varphi \equiv N(\sigma/D)^2$, ($0.03 \leq \varphi \leq 0.79$).

3 Particle tracking

A Phantom VEO 410L high speed camera has been used [3]. This model is capable of recording at 5200 frames per second at its maximum resolution (1280×800 pixels). At this resolution, we have recorded for each experiment a 99.92 s clip at 250 frames/s (well below the maximum operational speed of our camera). For low particle densities ($\varphi < 0.20$) three clips have been taken for each set of parameters (which improves the statistics of the data). Before each take the system has been thermalized for a few minutes, in order to assure steady state conditions (transient regime is very short for granular gas systems in most cases [22]).

We have developed a custom detection algorithm, where we combine the use of the open source library OpenCV [17] for particle detection together with TrackPy [2] (a python version of the Crocker and Grier algorithm [6]) for linking particle positions. Only a central region of interest (ROI) has been used for our subsequent analysis. This is done to minimize eventual boundary effects [11,1]. Our ROI is rectangular and has dimensions $L_x = 9.6 \sigma$, $L_y = 7.7 \sigma$.

3.1 Error estimation

Static localization error is defined as the standard deviation from the position of a motionless particle [4,13,20]. In order to quantify this static error, we recorded five videos with a single static sphere (fan switched off), positioned at different points of the system in each one. Measuring the deviation from the mean position, we have found this static error to be $\epsilon_s = 0.059$ pixels or, in units of the particle diameter, $\epsilon_s = 7.6 \times 10^{-4} \sigma$. Additionally, there are other factors that can have an effect on the quality of measurements, such as motion blur –also called dynamic error– [18]; this is due to the fact that cameras take a certain amount of time Δt to acquire each frame. In our particular case we used $\Delta t = 1.5 \times 10^{-3} \text{ s}$. Therefore, the positions that we obtain are not instantaneous, but averaged over that short period of time. This error has implications, for example, in determining the value of the diffusion coefficient D , and introducing uncertainty in the mean squared displacement (MSD) measurement [4]. Since we do not discuss here dynamical properties with characteristic times shorter than our Δt , this dynamic error can be neglected in the present work.

3.2 Isotropy and homogeneity conditions

In order to analyze the degree of isotropy in the collective dynamics, we have looked at the position distribution for x and y coordinates. Results are plotted

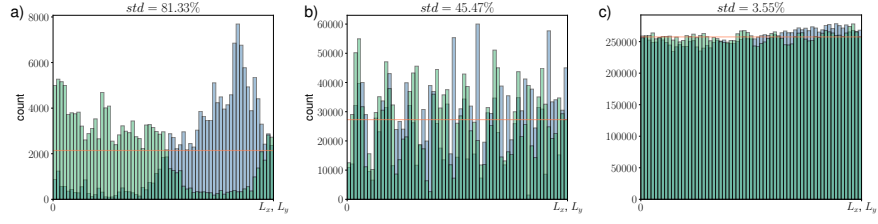


Fig. 2. Histogram of particle locations in the x (blue) and y (green) directions, during full-length clips for: (a) a system with a low packing fraction ($\varphi = 0.03$, $u_{air} = 4.63$ m/s), here particles remain near their initial positions; (b) a case in which packing fraction approaches a crystallization regime ($\varphi = 0.69$, $u_{air} = 2.80$ m/s), the reason behind the histogram maxima is that particles organize in a lattice structure. And (c), combined data for all the experiments recorded at intermediate densities, for which an isotropic liquid state is found ($0.20 \leq \varphi \leq 0.54$).

as histograms in Figure 2. We observed that except for very low (Figure 2a) or very high particle densities (Figure 2b), particles are evenly allocated throughout the surface, as seen in Figure 2c, with a standard deviation never greater than 5% [19]. In the case of high packing fractions, evidences of crystallization show up in the form of sharp and evenly distributed peaks (Figure 2b). On the other hand, at very low densities (Figure 2a), granular temperature is so low that the particles rarely move far away from their initial positions, thus skewing the distribution towards those regions.

With respect to the velocity distributions, and contrary to what happens with positions, we did not detect different behaviours depending on the packing fraction. Therefore, we represent in Figures 3a and 3b x and y velocity distribution functions respectively, combining the data from all of the clips altogether (we analyze in this way the *global isotropy of the set-up* rather than the isotropy of a particular experiment). We have observed that distribution functions in v_x and v_y are not Gaussian, which agrees with previous observations in granular dynamics experiments [16]. In any case, our velocity distributions are rather well centered at zero (mean values $\mu_x = 4.32 \times 10^{-3} \sigma/s$ and $\mu_y = 8.56 \times 10^{-3} \sigma/s$) and both have a similar standard deviation ($\sigma_x = 1.06 \sigma/s$ and $\sigma_y = 1.07 \sigma/s$), which is an indication of a high degree of horizontality. In addition, we represent in Figure 3c the particle speed modulus global distribution function $v = (v_x^2 + v_y^2)^{1/2}$, with mean value $1.22 \sigma/s$ and standard deviation $0.88 \sigma/s$. It is interesting to notice that a Gamma probability distribution ($f(x) = x^{a-1}e^{-x}/\Gamma(a)$ with shape parameter $a = 1.863$, in this case) provides a much better fit than a Maxwell-Boltzmann one.

In Figure 2 velocities are deduced from to frame-to-frame displacements. Let us analyze now the distribution of displacements at longer times. For this, we have determined the distribution function for 200-frames displacements, $\mathbf{d}_{200} = \mathbf{r}(t + 200) - \mathbf{r}(t)$, over the entire length of each experiment (of about 10^2 s); i.e., we have of the order of 2.5×10^4 events per particle. Would anisotropy occur, it

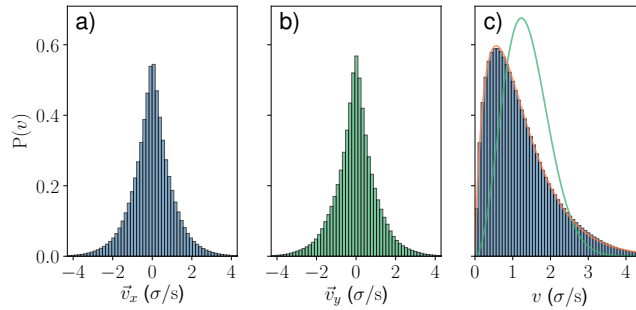


Fig. 3. Probability distribution function for the velocity of particles in the whole series of experiments. Displacements in the (a) x direction, (b) y direction, and (c) modulus of the velocity; for reference, gamma (orange) and Maxwellian (green) distribution fits are represented.

should show up in a polar coordinate representation (as in Figure 4b) in the form of a well defined maximum in the preferential displacement direction. We have selected a 200 frames window (this is roughly the time at which, at intermediate densities, particles 'forget' in our set-up their initial velocity, as calculated from the velocity autocorrelation function [12]). Figure 4b reveals a high degree of displacements isotropy. Figure 4a displays the histogram of particle positions for the same experiment. Interestingly, this representation reveals very clearly a hexagonal crystal structure.

4 Discussion

We have studied in this work a system of ping-pong balls thermalized by means of turbulent air wakes. The air current is adjusted so that balls are in contact with the table at all times (i.e., their movement is primarily two-dimensional). In the first part of this work, we have analyzed the accuracy of our experimental methods for particle tracking. As in previous works by other authors [4,13,20], we have made distinction between inherent static and dynamic errors, finding that in both cases they are very small. Homogeneity of particle density indicates that we achieved a good degree of horizontality in of our set-up (this work is intended to study only inhomogeneity-free dynamics). For intermediate densities, the degree of isotropy is very high (Figures 2c and 3). It is very interesting to remark that the distribution function of v (averaged over all of the series) fits a gamma distribution [10].

At high densities, it is interesting to notice the remnants of what seems to be a hexagonal crystal structure (Figures 2b and 4a). Phase transitions that can eventually appear in this system will be studied in more detail in an impending work.

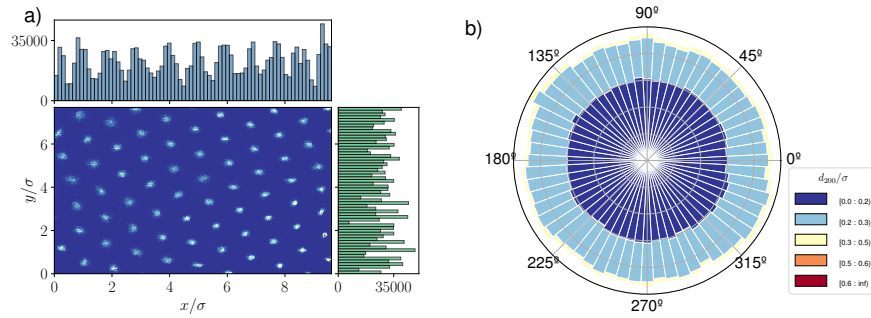


Fig. 4. Experiment with packing fraction $\varphi = 0.67$ and air flow velocity $u = 2.80$ m/s. (a) Particle positions histograms (upper and left panels) and plot of particle positions superimposed for all frames (central panel). A crystalline structure is clearly visible. (b) Stacked histogram in polar coordinates of 200 frame displacements (d_{200}) for that same system; different colours represent different displacement lengths (in units of the particle diameter). The histogram strongly suggests that particle dynamics is highly isotropic.

Acknowledgments

The authors thank J. S. Urbach, E. Abad and S. B. Yuste for fruitful discussions. We acknowledge funding from the Government of Spain through project No. FIS2016-76359-P and from the regional Extremadura Government through projects No. GR18079 & IB16087, both partially funded by the ERDF.

References

1. Abate, A.R., Durian, D.J.: Approach to jamming in an air-fluidized granular bed. *Phys. Rev. E* **74**(3), 1–12 (2006)
2. Allan, D. *et al.*: soft-matter/trackpy: Trackpy v0.4.2 (2019). DOI 10.5281/zenodo.3492186. URL <https://doi.org/10.5281/zenodo.3492186>
3. Ametek: Phantom high speed. URL <https://www.phantomhighspeed.com/products/cameras/veo>
4. Berglund, A.J.: Statistics of camera-based single-particle tracking. *Phys. Rev. E* **82**(1), 1–8 (2010)
5. Bragg, L., Nye, J.F.: A dynamical model of a crystal structure. *Proc. R. Soc. London A* **190**, 474 (1947)
6. Crocker, J.C., Grier, D.G.: Methods of digital video microscopy for colloidal studies. *J. Colloid Interface Sci.* **179**, 298–310 (1996)
7. Eaton, B.G., Finstad, R.G., Lane, P.D.: Kinetic theory simulator for laboratory use. *Am. J. Phys.* **47**, 132 (1979)
8. Finney, J.L.: Random packings and the structure of simple liquids. I. The geometry of random close packing. *Proc. R. Soc. London A* **319**, 479 (1970)
9. Friedel, J.: Dislocations. Pergamon, New York (1964)
10. Hogg, R.V., Craig, A.T.: Introduction to Mathematical Statistics, Sixth Edition. Macmillan Publishing Co., Inc, New York (1989)

11. Lanoiselée, Y., Briand, G., Dauchot, O., Grebenkov, D.S.: Statistical analysis of random trajectories of vibrated disks: Towards a macroscopic realization of Brownian motion. *Phys. Rev. E* **98**(6), 062,112 (2018)
12. M. A. López-Castaño, González-Saavedra, J.F., Rodríguez-Rivas, A., Abad, E., Yuste, S.B., Vega Reyes, F.: Diffusive properties of a system of macroscopic particles thermalized by turbulent air wakes (2019). In preparation
13. Ober, R.J., Ram, S., Ward, E.S.: Localization Accuracy in Single-Molecule Microscopy. *Biophys. J.* (2004)
14. Ojha, R.P., Lemieux, P.A., Dixon, P.K., Liu, A.J., Durian, D.J.: Statistical mechanics of a gas-fluidized particle. *Nature* **427**, 521 (2004)
15. Olafsen, J.A., Urbach, J.S.: Clustering, order and collapse in a driven granular monolayer. *Phys. Rev. Lett* **4369–4372**, 81 (1998)
16. Olafsen, J.S., Urbach, J.S.: Velocity distributions and density fluctuations in a granular gas. *Phys. Rev. E* **60**, R2468 (1999)
17. OpenCV: URL <https://opencv.org/>
18. Savin, T., Doyle, P.S.: Static and dynamic errors in particle tracking microrheology. *Biophys. J.* **88**(1), 623–638 (2005)
19. Scholz, C., Pöschel, T.: Velocity Distribution of a Homogeneously Driven Two-Dimensional Granular Gas. *Phys. Rev. Lett.* (2017)
20. Thompson, R.E., Larson, D.R., Webb, W.W.: Precise nanometer localization analysis for individual fluorescent probes. *Biophys. J.* (2002)
21. Van Dyke, M.: An album of fluid motion. The Parabolic Press, Stanford, CA, USA (1982)
22. Vega Reyes, F., Santos, A., Kremer, G.M.: Role of roughness on the hydrodynamic homogeneous base state of inelastic spheres. *Phys. Rev. E* **89**, 020,202(R) (2014)